

Excitonic spectra of wide parabolic quantum wells

Gerard Czajkowski, Sylwia Zielińska-Raczyńska, and David Ziemkiewicz^a

UTP University of Science and Technology, Bydgoszcz, Al. Prof. S. Kaliskiego 7, 85-789 Bydgoszcz, Poland

Received 30 March 2015 / Received in final form 1st July 2015

Published online 2 September 2015

© The Author(s) 2015. This article is published with open access at Springerlink.com

Abstract. The optical properties of wide quantum wells are considered, taking into account the screened electron-hole interaction potential and parabolic confinement potentials, different for the electrons and for the holes. The role of the interaction potential which mixes the energy states according to different quantum numbers is stressed. The results obtained by our method are in agreement with the observed spectra and give the possibility to the assessment of the resonances.

1 Introduction

We consider wide parabolic quantum wells (WPQW), of thicknesses in the growth direction of the order of a few excitonic Bohr radii of the well material. The structures with parabolic confinement have attracted more attention in the recent decades (for example, Refs. [1–15]). In typical (narrow) quantum wells (QW) with the dimension of, say, one excitonic Bohr radius in the growth direction we observe only a few excited states. The e-h Coulomb potential creates excitonic states below the fundamental gap, and the confinement increases the exciton binding energy. In WPQWs, due to the greater extension, significantly larger number of states is observed. The Coulomb potential and different confinement potentials for electrons and holes couples electron and hole confinement states of different quantum numbers. Such phenomena have been observed experimentally (see, for example, Ref. [1]). We propose the computational method which leads to analytical expression for the electric susceptibility of a wide parabolic quantum well taking into account the screened electron-hole interaction and parabolic confinement potential. The method is based on the so-called real density matrix approach (see, for example, Refs. [16–18]). With the purpose of exemplification, we consider a quantum well with GaAs as the optically active layer and Ga_{1-x}Al_xAs as the barriers, where the active layer is of the extension of a few excitonic Bohr radii. The absorption spectra of such a structure show a large number of resonances ($n = 8$ observed in Ref. [1]). The choice of optimal effective potential parameters as well as the damping constant used in our calculation is verified by numerical calculations of the total fitting error for maxima of susceptibility. We have chosen as reference the paper by Miller et al. [1] because it contains a lot of experimental data which allowed to compare the obtained theoretical results with experiment. The agree-

ment between our calculated spectrum and experimental data is very good with regard to the number and position of the maxima of susceptibility.

Our paper is organized as follows. In Section 2, we present the assumptions of considered model and solve the constitutive equation with an effective electron-hole interaction potential. Section 3 is devoted to the details of the applied potential. Next, in Section 4, the derived solution of constitutive equation is used to obtain the energy levels of the considered GaAs/Ga_{1-x}Al_xAs wide parabolic quantum well. Finally, in Section 5, the susceptibility for such nanostructure is calculated and discussed. The comparison of obtained results with experimental data and a brief overview of optimizing procedure is included.

2 The model

We will compute the linear optical response of a WPQW to a plain electromagnetic wave

$$E_i(z, t) = E_{i0} \exp(ik_0 z - i\omega t), \quad k_0 = \frac{\omega}{c}, \quad (1)$$

attaining the boundary surface of the WPQW active layer located at the plane $z = -L/2$. The second boundary is located at the plane $z = L/2$. The movement of the carriers in the z direction is determined by one-dimensional parabolic potentials, characterized by the oscillator energies $\hbar\omega_e, \hbar\omega_h$, respectively. We adopt the real density matrix approach to compute the optical properties. In this approach the linear optical response will be described by a set of coupled equations: two constitutive equations for the coherent amplitudes $Y_\nu(\mathbf{r}_e, \mathbf{r}_h)$, $\nu = H, L$ stands for heavy-hole (H) and (L) light-hole exciton; from them the polarization can be obtained and used in Maxwell's field equations. Having the field we can determine the QW optical functions (reflectivity, transmission, and absorption).

^a e-mail: david.ziemkiewicz@utp.edu.pl

Thus the next steps are the following: we formulate the constitutive equations. The equations will be then solved giving the coherent amplitudes Y . From the amplitudes we compute the polarization inside the quantum well, the electric field of the wave, and the optical functions. This scheme will be applied for the case investigated in reference [1].

As was explained in, for example, reference [18], the constitutive equation for the coherent amplitude Y in a quantum well has the form

$$\left[E_g - \hbar\omega - i\Gamma + \frac{\hat{p}_{ez}^2}{2m_e} + \frac{\hat{p}_{hz}^2}{2m_h} + \frac{\hat{p}_\rho^2}{2\mu_\parallel} + \frac{\hat{p}_\parallel^2}{2M_\parallel} + V_{eh}(\rho, z_e, z_h) + V_{\text{conf}}(z_e, z_h) \right] Y = \mathbf{M}(\mathbf{r})\mathbf{E}(\mathbf{R}), \quad (2)$$

where \mathbf{R} jest is the excitonic center-of-mass coordinate and $\mathbf{E}(\mathbf{R})$ is the electric field vector of the wave propagating in the QW; $V_{\text{conf}}(z_e, z_h)$ is the confinement potential for electrons and holes, and $\hat{p}_\rho, \hat{p}_\parallel$ are the momentum operators for the excitonic relative- and center-of-mass motion in the QW plane. The smeared-out transition dipole density $\mathbf{M}(\mathbf{r})$ is related to the bilocality of the amplitude $Y = Y(\mathbf{r}_e, \mathbf{r}_h)$ and describes the quantum coherence between the macroscopic electromagnetic field and the interband transitions. We assume for $\mathbf{M}(\mathbf{r})$ the form:

$$\mathbf{M}(\mathbf{r}) = \mathbf{M}(\rho, z, \phi) = \frac{\mathbf{M}_0}{2\pi\rho_0} \delta(z) \delta(\rho - \rho_0), \quad (3)$$

$z = z_e - z_h$ being the relative coordinate in the z direction, and ρ_0 is the so-called coherence radius [16,17]

$$\rho_0^{-1} = \sqrt{\frac{2\mu_\parallel E_g}{\hbar^2}}. \quad (4)$$

The above expression gives the coherence radius in terms of effective band parameters, but we find it convenient to treat the coherence radii as free parameters which can be determined by fitting experimental spectra. Mostly one takes it as a fraction of the respective excitonic Bohr radius.

In the following we assume that the propagating wave is linearly polarized in the x direction, and that the vector \mathbf{M} has a non-vanishing component in the same direction. Inserting the parabolic confinements we find in equation (2) Hamilton operators for the one-dimensional harmonic oscillator

$$H_e = \frac{\hat{p}_{ez}^2}{2m_e} + \frac{1}{2}m_e\omega_e^2 z_e^2, \quad H_h = \frac{\hat{p}_{hz}^2}{2m_h} + \frac{1}{2}m_h\omega_h^2 z_h^2. \quad (5)$$

Therefore we look for a solution Y in terms of the eigenfunctions of the operators H_e, H_h

$$Y(\rho, z_e, z_h) = \sum_{j,n=0}^N \psi_{ej}(z_e)\psi_{nh}(z_h)Y_{jn}(\rho). \quad (6)$$

The eigenfunctions ψ_j have the form

$$\psi_n(z) = \pi^{-1/4} \sqrt{\frac{\alpha}{2^n n!}} H_n(\alpha z) e^{-\frac{\alpha^2}{2} z^2}; \quad \alpha = \sqrt{\frac{m_z \omega}{\hbar}}, \quad (7)$$

with the Hermite polynomials $H_n(x)$ and parameters appropriate to electrons and holes, the corresponding eigenvalues are $E_n = (n + \frac{1}{2})\hbar\omega$. Substituting (6) into equation (2) we obtain equations for the functions Y_{jn}

$$\sum_{j,n=0}^N \left[E_g - \hbar\omega - i\Gamma + E_{je} + E_{nh} + \frac{\hat{p}_\rho^2}{2\mu_\parallel} + \frac{\hat{p}_\parallel^2}{2M_\parallel} + V_{eh}(\rho, z_e, z_h) \right] \psi_j(z_e)\psi_n(z_h)Y_{jn}(\rho) = \mathbf{M}(\mathbf{r})\mathbf{E}(\mathbf{R}). \quad (8)$$

Now we have to specify the shape of the interaction potential $V_{eh}(\rho, z_e, z_h)$ and the wave electric field $\mathbf{E}(\mathbf{R})$. We assume the so-called long-wave approximation and consider $\mathbf{E}(\mathbf{R})$ in equation (8) as a constant quantity. This approximation holds for nanostructures as for example, QWs, quantum dots, quantum wires, but cannot be applied for structures with larger extension in the z -direction, where the polaritonic aspect must be taken into account. The electron-hole interaction potential $V_{eh}(\rho, z_e, z_h)$ is, in general, the screened Coulomb potential

$$V_{eh}(\rho, z_e, z_h) = -\frac{e^2}{4\pi\epsilon_b \sqrt{\rho^2 + (z_e - z_h)^2}}, \quad (9)$$

ϵ_b being the dielectric constant of the QW material. Despite the nanostructures with cylindrical symmetry considered in reference [19], in the case of the wide QWs one does not have an orthonormal basis of functions so the use of an effective e-h interaction potential will be made

$$V_{eh} = -S \exp \left[-v(z_e - z_h)^2 - w\rho^2 \right], \quad (10)$$

where v, w are certain parameters which will be estimated below. Using the above potential, the dipole density (3), and neglecting the center-of-mass in plane motion, we put the constitutive equation (2) into the form

$$\left(E_{rs} + \frac{\hat{p}_\rho^2}{2\mu_\parallel} \right) Y_{rs} - e^{-w\rho^2} \sum_{nj} V_{rsnj} Y_{nj} = E \frac{M_0}{2\pi\rho_0} \langle r|s \rangle \delta(\rho - \rho_0), \quad (11)$$

where

$$E_{rs} = E_g + E_{re} + E_{sh} - \hbar\omega - i\Gamma, \quad (12)$$

$$V_{rsnj} = S \langle rs | \exp \left[-v(z_e - z_h)^2 \right] | nj \rangle \quad (13)$$

$$r, s, = 0, 1, 2, \dots,$$

with regard to the shape of the functions ψ only states of the same parity will give nonvanishing elements $\langle r|s \rangle$ so the states $|0e0h\rangle, |0e2h\rangle, |1e3h\rangle$, etc. will be taken into account. To summarize in order to calculate the optical response of a wide quantum well it is necessary to solve the constitutive equation (11) using the matrix elements $\langle r|s \rangle$ and the potential matrix elements (13).

3 The parameters of the effective potential

The further calculations require the estimation of parameters characterizing the effective potential (10). We make the following assumptions: (1) the potential is isotropic, in analogy to the Coulomb potential in isotropic materials. The nanostructure anisotropy is included in the quasiparticles effective masses. This assumption leads to the equality $v = w$. (2) We assume the value $S \approx 2R^*$ (R^* being the effective excitonic Rydberg energy for the given crystal); the exact value S will be established later. We determine the ground state energy of a hydrogen-like atom, where the interaction between the charges is given by equation (10). To this end we solve the Schrödinger equation

$$-\frac{\hbar^2}{2\mu} \left(\frac{d^2}{dr^2} + \frac{2}{r} \frac{\partial}{\partial r} \right) \psi - SR^* e^{-vr^2} \psi = E\psi. \quad (14)$$

Making use of the relation $\frac{\hbar^2}{2\mu} = R^* a^{*2}$ with the effective Bohr radius a^* , we introduce scaled variables

$$\rho = \frac{r}{a^*}, \quad \varpi = wa^{*2}, \quad \varepsilon = \frac{E}{R^*}, \quad (15)$$

transforming equation (14) to $H\psi = \varepsilon\psi$ with the Hamiltonian

$$H = - \left(\frac{d^2}{d\rho^2} + \frac{2}{\rho} \frac{d}{d\rho} \right) - S e^{-\varpi\rho^2}. \quad (16)$$

The considered Schrödinger equation will be solved by the variational method. Using the trial function $\psi = \exp(-\lambda\rho^2/2)$, we arrive at

$$\varepsilon(\lambda) = \frac{3}{2}\lambda - S \left(\frac{\lambda}{\lambda + \varpi} \right)^{3/2}. \quad (17)$$

By assuming the condition $\varepsilon = -1$ (which means that we want to reproduce the lowest exciton energy) and the vanishing derivative $\varepsilon' = 0$, one obtains a system of equations:

$$\begin{aligned} \frac{3}{2}\lambda - S \left(\frac{\lambda}{\lambda + \varpi} \right)^{3/2} &= -1, \\ \frac{1}{S} - \frac{\varpi}{\lambda^2} \left(1 + \frac{\varpi}{\lambda} \right)^{-5/2} &= 0. \end{aligned} \quad (18)$$

Therefore, only one of the values S , ϖ , λ is left as a free parameter. By taking, for example, $\varpi = 0.1$, one obtains $\lambda \approx 0.34$ and $S \approx 2.22$. These initial values will be refined by comparing the obtained excitonic spectra with the experimental data of Miller et al. [1]. These constants will be then used to determine the elements (13). In order to compute the optical spectra we have to solve the system (11) of coupled differential equations. This is a complicated task. We will simplify it by an approximation, which enables to transform equation (11) into a set of linear algebraic equations. This can be done in the following way. The terms $-V_{rsnj} \exp(-w\rho^2)$ play the role of effective e-h potentials, which determine the carriers motion in the xy -plane and lead to creation of bound excitonic states.

In the considered case the largest contribution to the optical spectra comes from the lowest exciton state, since the higher states have much smaller oscillator strengths. The exciton ground state is related to the potential matrix element V_{0000} . So we can assume, for a moment, that the equation with indices (0,0) decouples from the remaining equations. Then we obtain a single equation which can be easily solved and describe the motion in the xy plane. Denoting $V_{0000} = V_0$ we obtain the following equation for the amplitude Y_{00}

$$\left[H_1 + H_2 - V_0 e^{-w\rho^2} \right] Y_{00} = M_0 \frac{\delta(\rho - \rho_0)}{2\pi\rho_0} E \langle 0|0 \rangle, \quad (19)$$

where

$$\begin{aligned} H_1 &= E_g + E_{0e} + E_{0h} - \hbar\omega - i\Gamma, \\ H_2 &= \frac{-\hbar^2}{2\mu_{\parallel}} \left(\frac{d^2}{d\rho^2} + \frac{1}{\rho} \frac{d}{d\rho} + \frac{1}{\rho^2} \frac{d^2}{d\phi^2} \right). \end{aligned} \quad (20)$$

After rescaling the spatial variables in the effective excitonic Bohr radius the above equation becomes

$$\begin{aligned} k_{00}^2 Y_{00} + \left(-\frac{d^2}{d\rho^2} - \frac{1}{\rho} \frac{d}{d\rho} - \frac{1}{\rho^2} \frac{d^2}{d\phi^2} - v_0 e^{-\varpi\rho^2} \right) Y_{00} \\ = \frac{2\mu_{\parallel}}{\hbar^2} M_0 E \frac{\delta(\rho - \rho_0)}{2\pi\rho_0} \langle 0e|0h \rangle, \end{aligned} \quad (21)$$

where now ρ denotes the scaled variable ρ/a^* , and

$$k_{00}^2 = \frac{E_g + E_{0e} + E_{0h} - \hbar\omega - i\Gamma}{R^*}, \quad v_0 = \frac{V_0}{R^*}. \quad (22)$$

Assuming the s -symmetry for the ground state, we first solve the Schrödinger equation

$$\left(-\frac{d^2}{d\rho^2} - \frac{1}{\rho} \frac{d}{d\rho} - v_0 e^{-\varpi\rho^2} \right) \psi = \varepsilon\psi. \quad (23)$$

Using the variational method we solve the above equation, using the normalized trial function

$$\psi_0(\rho, \phi) = \frac{\sqrt{2\lambda}}{\sqrt{2\pi}} e^{-\lambda\rho^2/2}. \quad (24)$$

The variational scheme yields the value of λ which will be used below.

4 The solution of the constitutive equation

Making use of the above calculated function ψ_0 , we put the amplitude (6) into the form

$$Y(\rho, z_e, z_h) = \psi_0(\rho) \sum_{j,n=0}^N \psi_{ej}(z_e) \psi_{nh}(z_h) Y_{jn}, \quad (25)$$

where now Y_{jn} are constant coefficients. After rescaling the spatial variable $\rho \rightarrow \rho/a^*$ and using the quantities $k_{rs}^2 = \frac{E_{rs}}{R^*}$, $v_{rsnj} = \frac{V_{rsnj}}{R^*}$ we put equation (11) into the form

$$(k_{rs}^2 + \epsilon_0) Y_{rs} + v_{0000} \frac{\lambda}{\lambda + \varpi} Y_{rs} - \frac{\lambda}{\lambda + \varpi} \sum_{nj} v_{rsnj} Y_{nj} = \frac{2\mu_{\parallel}}{\hbar^2} EM_0 \langle er | hs \rangle \psi_0(\rho_0). \quad (26)$$

We obtained a system of linear algebraic equations for the coefficients Y_{nj} . Having them, we determine the amplitude Y (or amplitudes, when accounting the heavy – and light hole excitons H and L). Given the amplitude, we compute the polarization inside the quantum well and the electric field.

The described method can be used when we define the confinement energies $\hbar\omega_e, \hbar\omega_h$ and thus the parameters α_e, α_h . We will choose them to compare our theoretical results with the experimental findings of Miller et al. [1]. They obtained spectra for GaAs(Well)/Ga_{0.7}Al_{0.3}As (Barrier) QWs of three thicknesses: $L = 51 \pm 3.5$ nm, $L = 32.5 \pm 3.5$ nm, $L = 33.6 \pm 3.5$ nm. It can be noticed the uncertainty in determining the well thickness. The confinement parameters are obtained as follows. We consider a symmetric QW with a rectangular confinement potential

$$V = E_g(\text{Ga}_{0.7}\text{Al}_{0.3}\text{As}) - E_g(\text{GaAs}) = 482.8 \text{ meV}, \quad (27)$$

see Table 1. The confinement potentials for electrons V_e and holes V_h are chosen as:

$$\begin{aligned} V_e &= 0.85 V = 410.38 \text{ meV}, \\ V_h &= 0.15 V = 72.42 \text{ meV}. \end{aligned} \quad (28)$$

For the further calculations we have chosen the well of GaAs thickness $L = 51$ nm and computed the lowest energy states in the QW with potentials V_e, V_h , obtaining for the electron $E_{e0} = 21.78$ meV, $E_{h0zH} = E_{h0H} = 4.23$ meV for the heavy-hole and $E_{h0zL} = E_{h0L} = 17.20$ meV for the light hole (for the calculation scheme see, for example, [20,21]).

Thus the lowest confinement energy for the pair electron-heavy hole results

$$E_{0zH} = E_{e0z} + E_{h0zH} = 21.78 + 4.23 = 26.01 \text{ meV} \quad (29)$$

and for the pair electron-light hole

$$E_{0zL} = E_{e0z} + E_{h0zL} = 21.78 + 17.20 = 38.98 \text{ meV}. \quad (30)$$

Now we identify the confinement energies with the lowest parabolic confinement energies:

$$E_{e0} = \frac{\hbar\omega_e}{2}, \quad E_{h0} = \frac{\hbar\omega_h}{2}, \quad (31)$$

and obtain the confinement parameters α

$$\alpha_e a_H^* = \alpha_H^* \sqrt{\frac{m_e \omega_e}{\hbar}} = \sqrt{\frac{m_e}{\mu_{\parallel H}} \frac{E_{e0}}{R_H^*}} = 3.07, \quad (32)$$

$$\alpha_h a_H^* = \sqrt{\frac{m_{hzH}}{\mu_{\parallel H}} \frac{E_{h0H}}{R_H^*}} = 3.08. \quad (33)$$

Table 1. Band parameter values for GaAs, AlAs, and Ga_{0.7}Al_{0.3}As, AlAs data from [22], for Ga_{0.7}Al_{0.3}As by linear interpolation. Energies in meV, masses in free electron mass m_0 , γ_1, γ_2 are Luttinger parameters.

Parameter	GaAs	AlAs	Ga _{0.7} Al _{0.3} As
E_g	1519.2	3130	2002
m_e	0.0665	0.124	0.084
γ_1	6.85	3.218	
γ_2	2.1	0.628	
$m_{h\parallel H}$	0.112	0.26	
$m_{h\parallel L}$	0.210	0.386	
$\mu_{\parallel H}$	0.042		
$\mu_{\parallel L}$	0.05		
m_{hzH}	0.38	0.51	0.39
m_{hzL}	0.09	0.22	0.13
R_H^*	3.64	13.32	
R_L^*	4.3	19.35	
R_e^*	5.76		
a_H^*	15.78	7.03	
a_L^*	13.265	4.84	
a_e^*	9.97		
ϵ_b	12.53	11.16	12.12

with analogous calculations for the light hole. For the pair electron-heavy hole (heavy-hole exciton) we obtain

$$\begin{aligned} v_{0000H} &= \frac{V_{0000}}{R_H^*} = 2 \frac{(\tilde{\alpha}_{eH} \tilde{\alpha}_{hH}) \tilde{\alpha}_{eH}^2}{\tilde{\alpha}_{eH}^2 + \tilde{\alpha}_{hH}^2} \\ &\times \left[\frac{\tilde{\alpha}_{eH}^4}{\tilde{\alpha}_{eH}^2 + \tilde{\alpha}_{hH}^2} \left(\frac{\tilde{\alpha}_{eH}^2 \tilde{\alpha}_{hH}^2}{\tilde{\alpha}_{eH}^2 + \tilde{\alpha}_{hH}^2} + \varpi \right) \right]^{-1/2} \end{aligned} \quad (34)$$

where

$$\tilde{\alpha}_{eH} = a_H^* \alpha_e, \quad \tilde{\alpha}_{hH} = a_H^* \alpha_h. \quad (35)$$

Making use of equations (32) and (33), and putting $\varpi = 0.1$, we obtain $v_{0000} = v_0 = 1.98$. Then we obtained (see Ref. [21]) $\lambda = 0.545$, and the lowest heavy-hole exciton energy $\epsilon_{0H} = -1.128$. The lowest absorption peak observed in reference [1] corresponds to the energy 1535 meV, and the highest at about 1750 meV. Our calculations give the lowest heavy-hole exciton energy at

$$\begin{aligned} E_g + E(e0) + E(h0) + \epsilon_{0H} R_H^* \\ = E_g + E_{e0} + E_{h0H} + \epsilon_{0H} R_H^* \approx 1541 \text{ meV}. \end{aligned} \quad (36)$$

The resonance at 1750 meV will be obtained for the state $|e4h4\rangle$, i.e.

$$\begin{aligned} E_g + \left(4 + \frac{1}{2}\right) \hbar\omega_e + \left(4 + \frac{1}{2}\right) \hbar\omega_h + \epsilon_{0H} R_H^* \\ = E_g + 9(E_{e0} + E_{h0H}) + \epsilon_{0H} R_H^* \approx 1749 \text{ meV}. \end{aligned} \quad (37)$$

The lowest resonance for the light-hole exciton is at energy

$$\begin{aligned} E_g + E(e0) + E(h0) + \epsilon_0 \\ = E_g + E_{e0} + E_{h0L} + \epsilon_{0L} R_L^* \approx 1553 \text{ meV}. \end{aligned} \quad (38)$$

Table 2. Enumeration of states.

$ e0h0\rangle \rightarrow 1\rangle$	$ e1h1\rangle \rightarrow 2\rangle$	$ e2h2\rangle \rightarrow 3\rangle$
$ e3h3\rangle \rightarrow 4\rangle$	$ e4h4\rangle \rightarrow 5\rangle$	$ e0h2\rangle \rightarrow 6\rangle$
$ e0h4\rangle \rightarrow 7\rangle$	$ e1h3\rangle \rightarrow 8\rangle$	$ e2h0\rangle \rightarrow 9\rangle$
$ e2h4\rangle \rightarrow 10\rangle$	$ e3h1\rangle \rightarrow 11\rangle$	$ e4h0\rangle \rightarrow 12\rangle$
$ e4h2\rangle \rightarrow 13\rangle$		

whereas for the state $|e2h2\rangle$ we have

$$E_g + \left(2 + \frac{1}{2}\right) \hbar\omega_e + \left(2 + \frac{1}{2}\right) \hbar\omega_h + \varepsilon_{0L} R_L^* \\ = E_g + 5(E_{e0} + E_{h0L}) + \varepsilon_{0L} R_L^* \approx 1709 \text{ meV}. \quad (39)$$

Thus we conclude that the resonances observed in reference [1] come from the confinement states labeled by quantum numbers 0, 1, 2, 3, 4. As it follows from the relations (11), (12), and (13), the nonvanishing elements $\langle er|hs\rangle$ will be obtained for the confinement functions of the same parity, it means that either $r = 2k, s = 2m; k, m = 0, 1, 2$ or $r = 2k + 1, s = 2m + 1$. The same holds for the potential matrix elements. With regard to this property we choose the following 13 electron-hole states with appropriate renumbering (both for heavy- and light-hole exciton) displayed in Table 2 where the notation means, for example $|e2h0\rangle = \psi_{e2}(z_e)\psi_{h0}(z_h)$, etc. The same operation is performed for energies for light and heavy hole excitons

$$E_g + E_{er} + E_{hs} - \hbar\omega - i\Gamma \rightarrow E_{jhh}, \\ E_g + E_{er} + E_{ls} - \hbar\omega - i\Gamma \rightarrow E_{jhl}, \\ j = 1, 2, \dots, 13. \quad (40)$$

The potential matrix elements become now a square matrix

$$V_{rsnj} = \langle er|hs\rangle \exp[-v(z_e - z_h)^2] \langle eh|nj\rangle \rightarrow V_{jl}. \quad (41)$$

Using this notation we transform equations (26) into a system of linear equations for the 13 unknown quantities \mathcal{Y}_j

$$(k_j^2 + \varepsilon_0)\mathcal{Y}_j + v_{11} \frac{\lambda}{\lambda + \varpi} \mathcal{Y}_j - \frac{\lambda}{\lambda + \varpi} \sum_n v_{jn} \mathcal{Y}_n = b_j \quad (42)$$

where

$$b_j = \frac{\Delta_{LT}}{R^*} \langle er|hs\rangle \psi_0(\rho_0), \quad \frac{2M_0}{\varepsilon_0 \varepsilon_b \pi a^*} Y_{rs} = \mathcal{Y}_{rs} \cdot E, \quad (43)$$

with Δ_{LT} being the longitudinal-transversal splitting energy.

5 Results for GaAs/Ga_{1-x}Al_xAs parabolic quantum well and discussion

Solving equations (42), we have computed the optical functions of a GaAs/Ga_{1-x}Al_xAs parabolic quantum well

with a chosen total thickness of 51 nm. The values of the relevant parameters are well known, and are given in Table 1. In our scheme the polarization inside the QW is related to the coherent amplitudes by the relation

$$P(z) = 2M_0\psi_0(\rho_0) \sum_{j,n=0}^N |ejhn\rangle(z) Y_{jn}, \quad (44)$$

with the notation

$$|ejhn\rangle(z) = \psi_{ej}(z)\psi_{hn}(z). \quad (45)$$

Having the polarization, we compute the mean dielectric susceptibility

$$\bar{\chi} = \pi \varepsilon_b \psi_0(\rho_0) \sum_{\ell=0}^N \mathcal{Y}_\ell \langle 1|\ell\rangle_{\Lambda/2} \quad (46)$$

where $\langle 1|\ell\rangle_{\Lambda/2} = \frac{1}{\Lambda} \int_{-\Lambda/2}^{\Lambda/2} |\ell\rangle(\zeta) d\zeta, \Lambda = \frac{L}{a^*}$. Having the susceptibility, one can compute, using the appropriate boundary conditions, the optical functions (reflectivity, transmission, and absorption). We choose the absorption, which is related to the effective dielectric function by the formula

$$\alpha = \frac{2\omega}{c} \text{Im} \sqrt{\varepsilon_b + \bar{\chi}}, \quad (47)$$

ε_b being the dielectric constant of the QW material. Now we can compare the theoretical absorption spectra obtained by equation (47) with the photoluminescence excitation spectra from reference [1].

We have computed the absorption coefficient for the described above wide parabolic QW of the thickness 51 nm. The first step was to determine the coefficients S, ϖ satisfying equations (18). Then, by using the potential partition (28) and the formerly obtained value v , we have computed the potential matrix elements V_{rsnj} and the matrix elements $\langle r|s\rangle$. Assuming a certain value of the coherence radius ρ_0 , we have determined the lowest excitonic eigenfunction ψ_0 . Finally, taking a certain value of the damping parameter Γ , we have solved the constitutive equation (11), obtaining the coherent amplitudes. From the amplitudes we have computed the mean dielectric susceptibility (46) and the absorption coefficient (47). The results for the real and imaginary part of the mean susceptibility of the considered QW are displayed in Figure 1. The parameters used in the calculations are listed in the figure caption. The arrows indicate the positions of absorption maxima from reference [1]. The good agreement of theory and experiment (both in positions of maxima and their oscillator strengths) can be seen. In general, we observe 17 resonance peaks, from which 15 can be identified with those observed in experiment. The detailed comparison with peaks enumerated by rising energy is shown in Table 3. We have chosen the parameters to obtain the best fit to the experimental results of reference [1]. The accuracy of the optimal choice of the effective potential parameters and damping can be tested in the following way. We have computed the total fitting error for the first 13 maxima as a function of the parameters S, ϖ, Γ and v

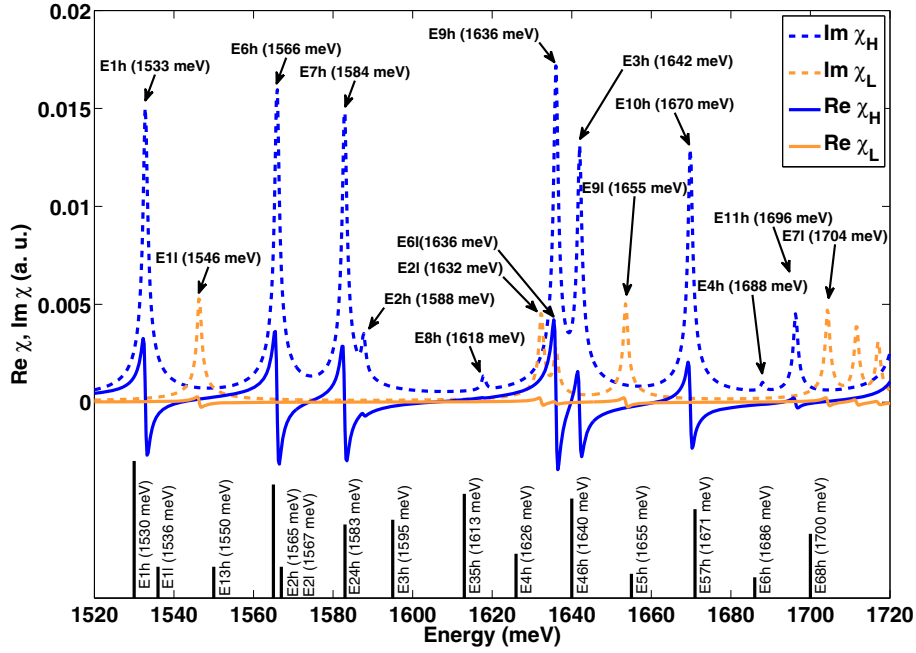


Fig. 1. The real and imaginary part of the mean QW susceptibility for the heavy-hole (H) and light-hole (L) exciton. The parameters used in calculations are $\varpi = 0.154$, $S = 2.6$, $v = 0.5$, $\Gamma = 0.5$ and the coherence radii $\rho_{0L} = 0.17 a_L^*$, $\rho_{0H} = 0.1 a_H^*$, respectively. The electron-hole states and their energies are assessed (indexed by 1, ..., 11) and the corresponding maxima from reference [1] are indicated below, with the heights of the bars indicating the oscillator strengths.

Table 3. The identification of the electron-hole states.

Number of maximum	State description	Nearest maximum from reference [1]
1	E1h (1533 meV)	E1h (1530 meV), E1l (1536 meV)
2	E1l (1546 meV)	E13h (1550 meV)
3	E6h (1566 meV)	E2h (1565 meV), E2l (1567 meV)
4	E7h (1583 meV)	E24h (1583 meV)
5	E2h (1588 meV)	E24h (1583 meV), E3h (1595 meV)
6	E8h (1618 meV)	E35h (1613 meV)
7	E2l (1632 meV)	E4h (1626 meV), E46h (1640 meV)
8	E9h (1636 meV)	E46h (1640 meV)
9	E6l (1636 meV)	E46h (1640 meV)
10	E3h (1642 meV)	E46h (1640 meV)
11	E9l (1654 meV)	E5h (1655 meV)
12	E10h (1671 meV)	E57h (1671 meV)
13	E4h (1688 meV)	E6h (1686 meV)
14	E11h (1696 meV)	E6h (1686 meV), E68h (1700 meV)
15	E7l (1704 meV)	E68h (1700 meV)

by changing the value of a single variable and computing the remaining ones according to system of equations (18). The results are shown in Figures 2a and 2b. We learned

that the positions of the absorption maxima is mainly affected by the values ϖ and S . One can see that the change the values of these parameters stretches the whole spectrum, causing a linear shift of the peak position, as shown on Figure 2c. When using the value $S = 2.6$, we obtain $\varpi \approx 0.154$, which represents a local minimum of fitting error. The assumed value of $v = 0.5$ is also a good choice. For the global minimum at $v = 1.2$, some parts of the absorption spectrum became negative, which was deemed unphysical. As expected, small values of Γ have no effect on the location of the peaks. For significant values of Γ , some peaks become indistinguishable, which is seen as a sudden jump in the fitting error. The selected parameter values gave the theoretical maxima close to the experimental values with mean error of less than 3.5 meV and enabled to identify the electron-hole states.

In the next step we tried to fit the experimental line shapes (oscillator strengths). We have observed that variations of the coherence radius change substantially the line-shapes. The best fit was obtained for $\rho_{0L} = 0.17 a_L^*$, $\rho_{0H} = 0.1 a_H^*$. It can be also verified that the increase of the damping parameter Γ results the lowering of the oscillator strength.

6 Conclusions

We have developed a simple mathematical procedure to calculate the optical functions of wide parabolic quantum wells. Our procedure describes the optical properties of a QW, taking into account the Coulomb interaction between electrons and holes. Our treatment includes anisotropic

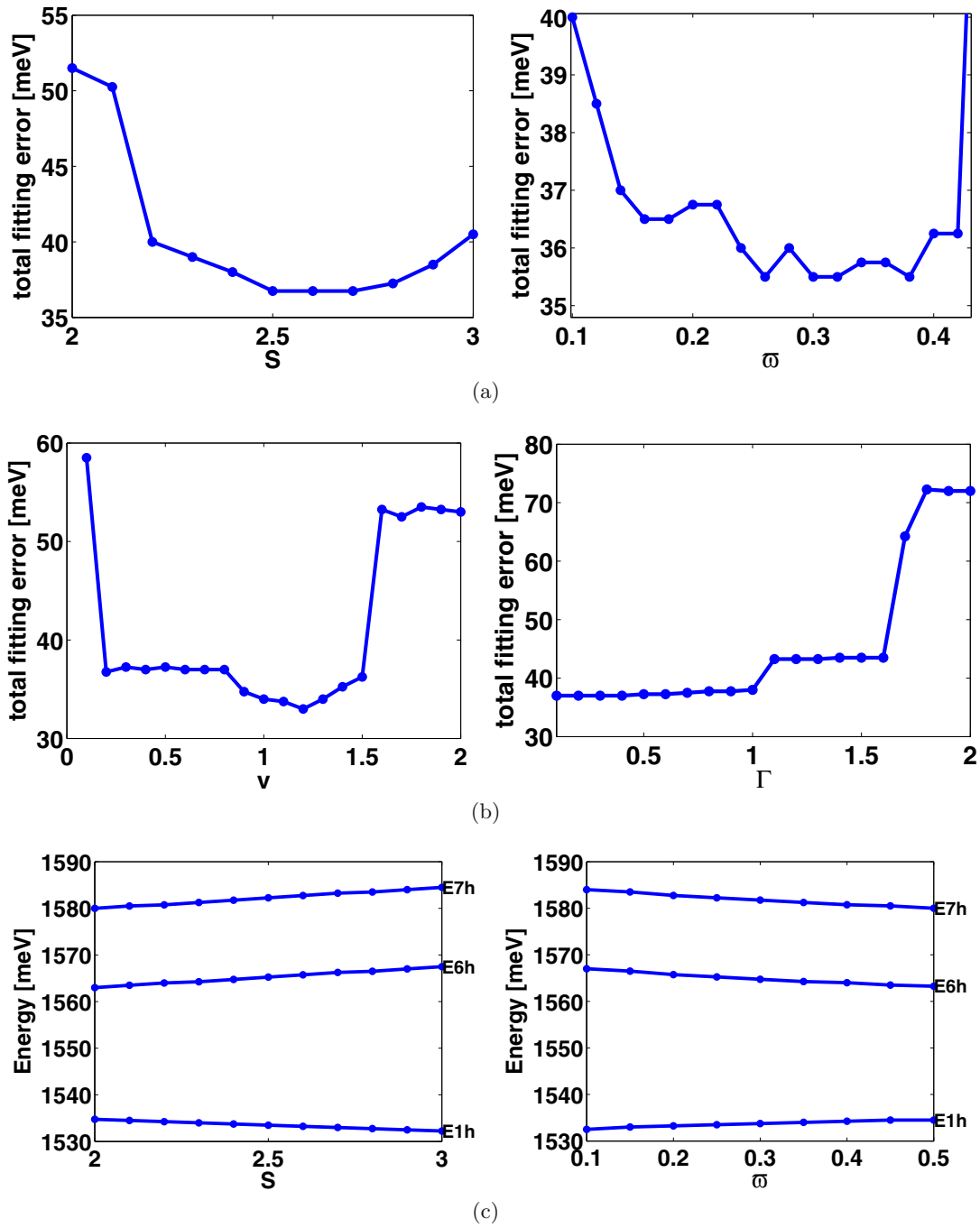


Fig. 2. The choice of the optimal calculation parameters. (a) Total fitting error as a function of S and ϖ . (b) Total fitting error as a function of ν and Γ . (c) The effect of the parameters S and ϖ on the position of the first three heavy hole exciton peaks.

properties of the QW, and takes into account coherence of the electron-hole pair with the radiation field. The presented method has been used to investigate the optical functions of GaAs/Ga_{1-x}Al_xAs parabolic quantum well for the case of radiation incidence parallel to the growth direction and it shows an excellent agreement with the experimental data, explaining the number and the positions of the absorption maxima. The justification of the choice of effective potential parameters and the damping constant is also presented.

References

1. R.C. Miller, A.C. Gossard, D.A. Kleinman, O. Munteanu, Phys. Rev. B **29**, 3740 (1984)
2. E.G. Gwinn, R.M. Westervelt, P.F. Hopkins, A.J. Rimberg, M. Sundaram, A.C. Gossard, Phys. Rev. B **39**, 6260 (1989)
3. L. Brey, N.F. Johnson, B.I. Halperin, Phys. Rev. B **40**, 10647 (1989)
4. K. Karraï, M. Stopa, X. Ying, H.D. Drew, S. Das Sarma, M. Shayegan, Phys. Rev. B **42**, 9732 (1990)

5. A. Wixforth, M. Sundaram, K. Ensslin, J.H. English, A.C. Gossard, *Phys. Rev. B* **43**, 10000 (1991)
6. M. Sundaram, S.J. Allen, Jr., M.R. Geller, P.F. Hopkins, K.L. Campman, A.C. Gossard, *Appl. Phys. Lett.* **65**, 2226 (1994)
7. H. Sari, Y. Ergün, I. Sökmen, *Superlatt. Microstruct.* **17**, 187 (1995)
8. Guo Kangxian, Chen Chuanyu, *Acta Photonica Sinica* **27**, 494 (1998)
9. N.A. El-Meshad, H.M. Hassanain, H.H. Hassan, *Egypt. J. Sol.* **24**, 1 (2001)
10. A. Matos-Abiague, *Semicond. Sci. Technol.* **17**, 150 (2002)
11. R.T. Senger, K.K. Bajaj, *Phys. Stat. Sol. B* **236**, 82 (2003)
12. G. Czajkowski, L. Skowroński, *Adv. Studies Theor. Phys.* **1**, 187 (2007)
13. A. Tabata, M.R. Martins, J.B.B. Oliveira, T.E. Lamas, C.A. Duarte, E.C.F. da Silva, G.M. Gusev, *J. Appl. Phys.* **102**, 093715 (2007)
14. A. Tabata, J.B.B. Oliveira, E.C.F. da Silva, T.E. Lamas, C.A. Duarte, G.M. Gusev, *J. Phys.: Conf. Ser.* **210**, 012052 (2010)
15. A. Taqi, J. Diouri, *Semicond. Phys. Quantum Electron. Optoelectron.* **15**, 21 (2012)
16. A. Stahl, I. Balslev, *Electrodynamics of the Semiconductor Band Edge* (Springer-Verlag, Berlin, Heidelberg, New York, 1987)
17. G. Czajkowski, F. Bassani, A. Tredicucci, *Phys. Rev. B* **54**, 2035 (1996)
18. G. Czajkowski, F. Bassani, L. Silvestri, *Rivista del Nuovo Cimento* **26**, 1 (2003)
19. P. Schillak, *Eur. Phys. J. B* **84**, 17 (2011)
20. J.H. Davies, *The Physics of Low-Dimensional Semiconductors* (Cambridge University Press, 1998)
21. G. Czajkowski, S. Zielińska-Raczyńska, D. Ziemkiewicz, [arXiv:1502.05329v1](https://arxiv.org/abs/1502.05329v1) [*cond-mat.mes-hall*] (2015)
22. M. Grundmann, O. Stier, D. Bimberg, *Phys. Rev. B* **52**, 11969 (1995)

Open Access This is an open access article distributed under the terms of the Creative Commons Attribution License (<http://creativecommons.org/licenses/by/4.0>), which permits unrestricted use, distribution, and reproduction in any medium, provided the original work is properly cited.